$$\left(\frac{\partial \ln \eta_{ij}}{\partial \ln T}\right)_{\tilde{v}} = -\frac{\Delta e_{ij}}{kT\tilde{v}} \exp\left(\frac{\kappa}{\tilde{v}}\right)\left[1 - \left(1+\frac{\kappa}{\tilde{v}}\right)\left(\frac{d \ln V^*}{d \ln T}\right)\right] - \frac{\Delta \sigma_{ij}'}{kT} \quad \text{(C8)}$$

where

$$\Delta e_{ij} = e_{ij} - \frac{e_{ii} + e_{jj}}{2} \quad \text{(C9)}$$

$$\Delta \sigma_{ij}' = \sigma_{ij}' - \frac{\sigma_{ii}' + \sigma_{jj}'}{2} \quad \text{(C10)}$$

The derivatives $(\partial \ln Y_i/\partial \ln \tilde{v})_T$ and $(\partial \ln Y_i/\partial \ln T)_{\tilde{v}}$ in Equation (C7) are found by solving simultaneous linear equations obtained by differentiating Equation (34) with respect to $\tilde{v}$ and T, respectively. Since the equations are similar, we will write them only in the case of $\tilde{v}$, and they are

$$\sum_j A_{ij} X_j' = -F_i' \quad \text{(C11)}$$

where

$$X_j' = \frac{\partial \ln Y_j}{\partial \ln \tilde{v}} \quad \text{(C12)}$$

and

$$F_i' = Y_i \sum_j a_{ij} Y_j \left(\frac{\partial \ln \eta_{ij}}{\partial \ln \tilde{v}}\right) \quad \text{(C13)}$$

Manuscript received September 7, 1976; revision received December 20, 1976, and accepted January 5, 1977.

Influence of Schmidt Number on the Fluctuations of Turbulent Mass Transfer to a Wall

DUDLEY A. SHAW

and

THOMAS J. HANRATTY

University of Illinois
Urbana, Illinois 61801

Measurements are presented on the influence of Schmidt number on the frequency of the mass transfer fluctuations at a solid boundary. The shape of the spectral function is similar at all Schmidt numbers. A relation between the mass transfer fluctuations and the fluctuating velocity field can be obtained only at high frequencies. A comparison of the scale and the frequency of the mass transfer fluctuations and the velocity fluctuations suggests that the rate of mass transfer is controlled by convective motions in the flow oriented eddies described by a number of previous investigators. However, the concentration fluctuations caused by these convective motions are greatly dampened close to the wall by molecular diffusion. Thus the mass transfer fluctuations reflect only the scale and not the frequency of the convective motions in the flow oriented eddies.

SCOPE

When mass is exchanged between a turbulent fluid and a solid boundary, the local rate of mass transfer varies erratically with time. In two previous studies from this laboratory (Van Shaw and Hanratty, 1964; Sirkar and Hanratty, 1970), the fluctuations in the rate of mass transfer to a pipe wall were measured in order to better understand the role that the turbulent convective motions play in the transfer process. It was found that mass transfer fluctuations are of much lower frequency than velocity fluctuations close to the wall and that the spatial extent of the mass transfer fluctuations is much smaller in the transverse direction than in the direction of flow.

In order to examine in greater detail how the concentration boundary layer dampens concentration fluctuations close to a wall, Shaw (1976) recently performed experiments in which he measured the spectral function and the spatial correlation functions characterizing the mass transfer fluctuations. The results of his studies and their implications with respect to modeling turbulent mass transfer to a solid boundary are presented in this paper.

Two general postulates proposed by Sirkar and Hanratty (1970) are used to relate the mass transfer fluctuations to the velocity fluctuations. One of these is the assumption that linear theory describes the high frequency mass transfer fluctuations. The other is a pseudo steady state assumption whereby the limiting behavior at low frequencies is described by a steady state form of the mass balance equation.

Correspondence concerning this paper should be addressed to Thomas J. Hanratty.

CONCLUSIONS AND SIGNIFICANCE

The average frequency of the mass transfer fluctuations at the wall is decreased with Schmidt number as $Sc^{-0.404}$ The spectral density function of the mass transfer fluctuations W_k is similar at different Schmidt numbers in that a plot of $(W_k)/(k^{+2}\,Sc^{0.41})$ vs. $nSc^{0.41}$ is not dependent on Schmidt number.

Further support is obtained for the relation of the mass transfer fluctuations to the velocity field developed by Sirkar and Hanratty for high frequencies, since it is found that this relation correctly describes the influence of Schmidt number, as well as of frequency, on W_k.

The time scale of the mass transfer fluctuations is too large for them to be associated with the temporal variation of the velocity field in the flow oriented wall eddies, as previously suggested by Sirkar and Hanratty. This presents an apparent paradox in that the scales characterizing the mass transfer fluctuations and the flow oriented eddies are of similar magnitudes.

The picture of the mass transfer process suggested to us from measurements is that the rate of mass transfer is controlled by the convective motions in the flow oriented eddies. Concentration fluctuations associated with these convective motions are greatly dampened by molecular diffusion close to the wall so that the scale but not the frequency of the flow fluctuations in the wall eddies is reflected in the mass transfer fluctuations. The mass transfer fluctuations actually observed at the wall could then be interpreted as due to the meandering of these flow oriented eddies and not the actual turbulent motions controlling the mass transfer process.

OUTLINE OF PREVIOUS WORK

All of the studies of mass transfer fluctuations at a wall have used an electrochemical technique which involves the measurement of the current to a wire embedded in, but electrically insulated from, the wall of a pipe section which is the cathode of an electrolysis cell. Van Shaw (1963) and Sirkar (1969) used an aqueous electrolyte system that involved the following redox reactions:

$$\text{cathode} \quad Fe(CN)_6^{3-} + e^- \rightarrow Fe(CN)_6^{4-}$$

$$\text{anode} \quad Fe(CN)_6^{4-} \rightarrow Fe(CN)_6^{3-} + e^-$$

Shaw (1976) used an aqueous iodine electrolyte in addition to the ferricyanide electrolyte:

$$\text{cathode} \quad I_3^- + 2e^- \rightarrow 3I^-$$

$$\text{anode} \quad 3I^- \rightarrow I_3^- + 2e^-$$

The cathode voltage was kept at a high enough value that the reduction of the active ion was mass transfer controlled. The current I flowing to the test electrode of area A is then related to the mass transfer coefficient by

$$K = \frac{I}{A\,F\,C_b\,n_e} \tag{1}$$

The solutions had a sufficient excess of neutral electrolyte to insure that the mass transfer rate was not influenced by electric field effects.

Van Shaw (1963) used a 2.54 cm diameter test section that contained test electrodes with diameters of 0.0404 to 0.318 cm. There was some uncertainty in the interpretation of his results because the scale of the mass transfer fluctuations in a 2.54 cm pipe is so small that the flow over a 0.0404 cm test electrode cannot be assumed uniform. For this reason, Sirkar (1969) carried out the same experiments in a 19.36 cm diameter pipe. He found that the spatial averaging is eliminated when the diameter of the electrode made dimensionless with respect to wall parameters $2a$ is less than 12. He showed that the intensity of the mass transfer fluctuations $(\overline{k^2})^{1/2}/\overline{K}$ at a Schmidt number of 2 300 had a value of 0.29 rather than the 0.48 that Van Shaw estimated by extrapolating measurements from electrodes of different size.

Shaw (1976) examined the influence of Schmidt number with the ferro-ferricyanide system by changing the concentration of sodium hydroxide and for the iodine system by adding sucrose. The experiments were carried out in a 2.54 cm diameter test section. The test electrodes were much smaller than those used by Van Shaw (1963) in order to insure that experiments were performed under conditions where averaging was not occurring over the electrode surface.

DESCRIPTION OF THE EXPERIMENTS

Flow System

The flow system and the experimental techniques used in this recent study by Shaw are described in a previous article (Shaw and Hanratty, 1976) in which results on average mass transfer rates are presented. Consequently, the discussion presented here is confined to aspects of the experiments which are particularly related to the measurement of the fluctuations in the mass transfer rates.

Test sections with lengths of 5.72 and 10.8 cm were used. Both were made from a 2.54 cm I.D. brass pipe that was platinum plated. After they were finished and plated, the inside diameters of the sections were 2.64 cm.

The test electrodes were fitted to short entry and exit sections of tubing. Great care was taken to insure that there were no discontinuities in the cross section of the pipe immediately upstream and downstream of the electrode.

The 5.72 cm electrode was used to determine the effect of wire size on the measured spectra. It contained eight wires of various sizes located 4.45 cm from the upstream edge and arranged around the circumference 10 deg apart. There were two wires of each of the following diameters: 0.0127, 0.0211, 0.0404, and 0.0643 cm. The 10.8 cm electrode, which contained twelve 0.0127 cm diameter platinum wires, was used to measure the spectra and the transverse correlations of the mass transfer coefficient. The wires were placed 9.53 cm from the upstream edge of the electrode and were arranged around the circumference with center to center positions of 2, 4, 6, 8, 13, 18, 23, 28, 38, 48, and 58 deg. from the first electrode.

Electrical Equipment

The basic circuit used for mass transfer measurements is shown in Fig. 1. An Analog Devices 180B operational amplifier, modified for use with large currents, operated as a current to voltage converter to measure the current to the pipe section. Each of the circular wire electrodes had its own circuit with an Analog Devices 118A operational amplifier.

The potential applied to the cathode was determined by the setting of the 1KΩ helipot. The applied potential

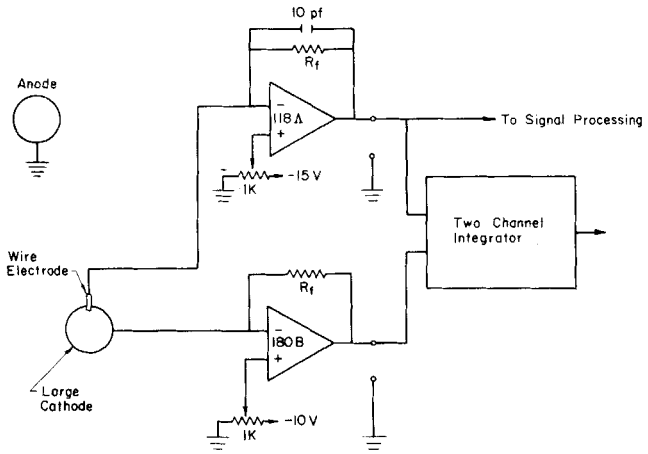

Fig. 1. Electronic circuit for mass transfer measurement.

at each wire was the same as the applied potential determined by the large electrode within ±2 mV measured on a digital voltmeter. Anodes upstream and downstream from the cathode were connected to the amplifier ground and to the building cold water line.

The signal from each wire electrode consisted of a time averaged and a fluctuating voltage. Before the signal was recorded on magnetic tape, the DC level was subtracted and the fluctuations were amplified by an analogue circuit described by Eckelman (1971). While the signal was being recorded, the mean square of the signal was determined by squaring the signal and integrating with analogue squaring circuits described in a thesis by Lee (1972).

The frequency spectra were measured with a Saicor SAI-52B digital spectrum analyzer/integrator. Since the signal consisted of very low frequencies, it was convenient to play back the recorded data at eight times the speed it was recorded. This reduced the amount of time needed to analyze the data.

The circumferential correlation coefficients were calculated with an IBM 1800 computer. A detailed description of the method can be found in a thesis by Eckelman (1971).

THEORY

Similarity Assumption

The spectral distribution function describing the mass transfer fluctuations is defined as

$$\overline{k^{+2}} = \frac{\overline{k^2}}{v^{*2}} = \int_0^\infty W_k \, dn \tag{2}$$

where W_k and n have been made dimensionless using wall parameters v^* and ν. From dimensional considerations, the following relation can be written for a fully developed concentration field:

$$W_k = f(n, Re, Sc). \tag{3}$$

Since the mass transfer fluctuations are influenced by velocity fluctuations close to the wall, it can be expected that a law of the wall will hold, whereby

$$W_k = g(n, Sc) \tag{4}$$

In this research we explored the similarity hypothesis that

$$\frac{W_k}{\overline{k^{+2}}\, Sc^p} = h(n\, Sc^p) \tag{5}$$

This implies that there is an exponent p for which a plot of $(W_k)/(\overline{k^{+2}}\, Sc^p)$ vs. $n\, Sc^p$ will produce a single curve independent of Schmidt number. The justification for this type of relation can be obtained only from experimental evidence to be presented later in the paper.

Mass Balance Equations

The concentration of the diffusing substance is represented as the sum of time averaged and fluctuating components $C = \overline{C} + c$. The mass balance equations for $\overline{C}$ and c for fully developed concentration and flow fields can be written as

$$\overline{U}\frac{\partial \overline{C}}{\partial x} = \frac{1}{Sc}\frac{\partial^2 \overline{C}}{\partial y^2} - \frac{\partial}{\partial y}(\overline{vc}) \tag{6}$$

$$\frac{\partial c}{\partial t} + \overline{U}\frac{\partial c}{\partial x} + v\frac{\partial \overline{C}}{\partial y} + u\frac{\partial \overline{C}}{\partial x} = \frac{1}{Sc}\left(\frac{\partial^2 c}{\partial x^2} + \frac{\partial^2 c}{\partial y^2} + \frac{\partial^2 c}{\partial z^2}\right) - \frac{\partial}{\partial x}(uc) - \frac{\partial}{\partial y}(vc - \overline{vc}) - \frac{\partial (wc)}{\partial z} \tag{7}$$

where all concentrations have been made dimensionless using the bulk concentration C_B and all lengths and velocities using wall parameters v^* and ν. Sirkar has shown that for $Sc = 2\,300$, the derivative $\partial\overline{C}/\partial x \simeq 10^{-7}$. Consequently, the terms $\overline{U}(\partial\overline{C})/(\partial x)$ and $u(\partial\overline{C})/(\partial x)$ can be neglected for large Schmidt numbers. In addition, Sirkar argued that for large Schmidt numbers the concentration boundary layer is thin enough that diffusion in the x and z directions can be neglected compared to diffusion in the y direction. The mass balance equations therefore simplify to

$$0 = \frac{1}{Sc}\frac{d^2\overline{C}}{dy^2} - \frac{d}{dy}(\overline{vc}) \tag{8}$$

$$\frac{\partial c}{\partial t} + \overline{U}\frac{\partial c}{\partial x} + v\frac{d\overline{C}}{dy} = \frac{1}{Sc}\frac{\partial^2 c}{\partial y^2} - \frac{\partial (uc)}{\partial x} - \frac{\partial}{\partial y}(vc - \overline{vc}) - \frac{\partial (wc)}{\partial z} \tag{9}$$

Since a very thin concentration boundary layer is being assumed, the velocity can be represented by expressions for its limiting behavior close to a wall:

$$\overline{U} = y \tag{10}$$

$$u = s_x(t,z,x)y \tag{11}$$

$$v = \frac{1}{2}\left(\frac{\partial s_x}{\partial x} + \frac{\partial s_z}{\partial z}\right) y^2 \tag{12}$$

$$w = s_z(t,z,x)y \tag{13}$$

The turbulent transport term $\overline{vc}$ can be represented by using the concept of an eddy diffusion coefficient

$$-\overline{vc} = \epsilon^+ \frac{d\overline{C}}{dy} \tag{14}$$

where, from the recent work by Shaw and Hanratty (1976), $\epsilon^+ = \epsilon/\nu$ is given by

$$\epsilon^+ = by^m \tag{15}$$

with $b = 0.000463$ and $m = 3.38$.

Equations for the average concentration field and for the mass transfer coefficient are obtained from (8) and (15) using the boundary conditions

$$\overline{C} = 0 \text{ at } y = 0$$

$$\overline{C} = 1 \text{ at } y = \infty \tag{16}$$

$$\overline{C} = \frac{m}{\pi} b^{1/m} \sin\left(\frac{\pi}{m}\right) Sc^{-\left(\frac{m-1}{m}\right)} \int_0^y \frac{dy}{\frac{1}{Sc} + by^m} \tag{17}$$

$$\overline{K_\infty}^+ = \frac{m}{\pi} b^{1/m} \sin\left(\frac{\pi}{m}\right) Sc^{-\left(\frac{m-1}{m}\right)} \tag{18}$$

where $\overline{K_\infty}^+$ signifies the fully developed mass transfer coefficient made dimensionless with respect to the friction velocity.

Solution for High Frequencies

We first explore the suggestion by Sirkar and Hanratty that the high frequency concentration fluctuations are given by a solution to a form of the mass balance equation linear in the fluctuating quantities

$$\frac{\partial c}{\partial t} + \overline{U}\frac{\partial c}{\partial x} + v\frac{d\overline{C}}{dy} = \frac{1}{Sc}\frac{\partial^2 c}{\partial y^2} \tag{19}$$

If the fluctuating concentration field has a wavelike behavior, then $\partial c/\partial t = U_c\,(\partial c)/(\partial x)$, where U_c is the convection velocity of the waves made dimensionless with respect to the friction velocity. Recent measurements of the fluctuating flow field close to a wall would suggest $U_c \cong 8$ (Morrison et al., 1971). Van Shaw made a rough estimate that for mass transfer fluctuations $U_c \cong 1$, so there is some uncertainty as to what to assume for U_c. For very high frequencies, the region over which molecular diffusion δ_c is important is small compared to the concentration boundary layer $\delta\,\overline{c}$. Consequently, the solution to (19) for $\omega \to \infty$ can be regarded as the composite of an outer solution which ignores molecular diffusion with length scale $\delta\,\overline{c}$ and an inner solution with length scale δ_c that includes its effect. If the matching point is close enough to the solid boundary that $d\overline{C}/dy$ may be taken as equal to its value at the wall $d\overline{C}/dy|_0 = \overline{K_\infty}^+ Sc$, and that $U_c >> \overline{U}$, then the solution for the mass flux at the wall presented by Sirkar and Hanratty (1970) can be used.

The differential equation describing the concentration field close to the wall is

$$\frac{\partial c}{\partial t} + v\frac{d\overline{C}}{dy}\bigg|_0 = \frac{1}{Sc}\frac{\partial^2 c}{\partial y^2} \tag{20}$$

The velocity field is represented by a function harmonic in time

$$v = \hat{v}\, y^2\, e^{i\omega t} \tag{21}$$

Since (20) is linear, its solution is given in the form

$$c = \hat{c}\,(y)\, e^{i\omega t} \tag{22}$$

The substitution of (21) and (22) into (20) yields the following relation for $\hat{c}$:

$$i\omega\hat{c} + \hat{v}y^2\frac{d\overline{C}}{dy}\bigg|_0 = \frac{1}{Sc}\frac{d^2\hat{c}}{dy^2} \tag{23}$$

This is to be solved from boundary conditions $\hat{c} = 0$ at $y = 0$. For large y, it is to be matched to the solution of

$$\frac{\partial c}{\partial t} + \overline{U}\frac{\partial c}{\partial x} + v\frac{d\overline{C}}{dy} = 0 \tag{24}$$

In the matching region, $\overline{U}\,(\partial c)/(\partial x)$ is small compared to $\partial c/\partial t$ so that the solution there is given as

$$\hat{c} = -\frac{\hat{v}y^2}{i\omega}\frac{d\overline{C}}{dy}\bigg|_0 \tag{25}$$

From the form of (23), it follows that the thickness of the region characterizing the inner solution depends on ω and Sc in the following way:

$$\delta_c^2 \sim (\omega Sc)^{-1} \tag{26}$$

From (26) it is clear that δ_c becomes vanishingly small compared to $\delta\,\overline{c}$ for $\omega \to \infty$.

Since (23) is linear, it follows that the spectral function of the mass transfer fluctuations, defined by Equation (2), can be derived from a solution to (23):

$$W_k = \hat{k}\,\hat{k}^* \tag{27}$$

where

$$\hat{k} = \frac{1}{Sc}\frac{d\hat{c}}{dy}\bigg|_0$$

and $\hat{k}^*$ is the complex conjugate of $\hat{k}$. If variables

$$\tilde{c} = \frac{\hat{c}\,\omega^2\, Sc}{\hat{v}\frac{d\overline{C}}{dy}\Big|_0} \quad \text{and} \quad \tilde{y} = y(\omega\, Sc)^{1/2}$$

are defined, (23) takes the form

$$i\tilde{c} + \tilde{y}^2 = \frac{d^2\tilde{c}}{d\tilde{y}^2} \tag{28}$$

with $\tilde{c} = 0$ at $\tilde{y} = 0$ and $\tilde{c} \to i\tilde{y}^2$ for large $\tilde{y}$. Since no parameters appear in (28) or in the boundary conditions, it follows that $d\tilde{c}/d\tilde{y}|_0$ is independent of Sc and therefore that $W_k \sim W_V\overline{K}^{+2}/Sc\,\omega^3$, where $W_V = \hat{v}\,\hat{v}^*$. From the solution of (28) presented by Sirkar, we find

$$W_k = \frac{4W_V\overline{K}^{+2}}{Sc\,\omega^3} \tag{29}$$

If (29) is put in the form of similarity variables defined previously, then

$$\frac{W_k}{\overline{k}^{+2}Sc^p} = \frac{4W_V}{\left[Sc^{\frac{(1+p)}{3}}\omega\right]^3}\frac{\overline{K^2}}{\overline{k^2}} \tag{30}$$

It follows that for both (28) and the similarity hypothesis to be correct at high frequencies

$$\frac{\overline{k^2}}{\overline{K^2}} \sim Sc^{(2p-1)} \tag{31}$$

or that the intensity of the mass transfer fluctuations should vary with Schmidt number unless $p = \frac{1}{2}$.

Low Frequency Solution

Sirkar (1969) has argued that for low frequencies the fluctuating concentration field should be described by a

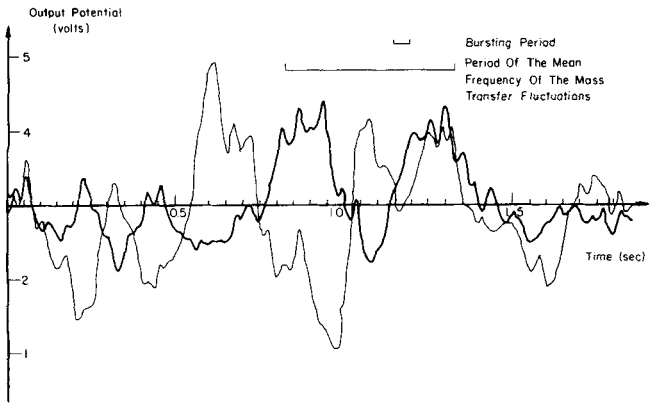

Fig. 2. Fluctuation of the turbulent mass transfer coefficient from two electrodes with circumferential spacing of 0.0457 cm. ($z = 18.1$).

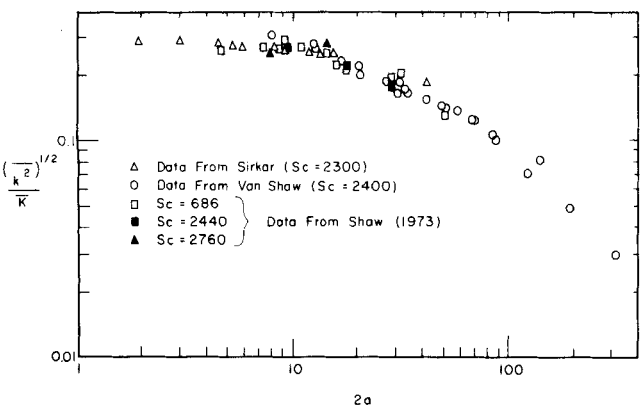

Fig. 3. Effect of electrode size on the intensity of mass transfer fluctuations.

pseudo steady state assumption, whereby the mass balance equations for the total concentration and the fluctuating concentration are given as follows for a flow field that is approximately homogeneous in the flow direction:

$$w\frac{\partial C}{\partial z} + v\frac{\partial C}{\partial y} = \frac{1}{Sc}\frac{\partial^2 C}{\partial y^2} \tag{32}$$

and

$$v\frac{d\overline{C}}{dy} - \frac{1}{Sc}\frac{\partial^2 c}{\partial y^2} = -\frac{\partial}{\partial y}(vc - \overline{vc}) - \frac{\partial(wc)}{\partial z} \tag{33}$$

with boundary conditions

$$C = C_B \quad c = 0 \; y \to \infty$$

$$C = c = 0 \; y = 0$$

It is to be noted that the simplification of (17) to (33) involves the neglect of the term $\partial(uc)/\partial x$ in addition to the time derivatives. This is justified because the scale of the turbulent fluctuating quantities in the direction of flow is so large. The chief difficulty in solving (33) is the evaluation of the terms which are nonlinear in the fluctuating quantities. Sirkar did this by solving (32) for a fluctuating velocity field which has a periodic variation in the z direction with wavelength equal to the scale of the streaky wall structures observed close to a wall by a number of investigators (see Lee et al., 1974). This approach now appears incorrect because the frequency of the mass transfer fluctuations is much smaller than the frequency of the velocity fluctuations of the flow oriented wall eddies responsible for the streaky structure.

Shaw (1976) has examined two alternate methods for utilizing the pseudo steady state assumption. In one of these, the nonlinear terms are neglected. In the other they are approximated by the term $d/dy\ (\epsilon + dc^+/dy^+)$, where ϵ^+ is the eddy diffusivity defined by (14). Both methods predict

$$\frac{W_1}{\overline{K^{+2}}} \sim Sc^{0.225} \tag{34}$$

for ϵ^+ given by (15) with $m = 3.38$. It will be shown later that the comparison of (34) with the Schmidt number dependency indicated by measurements is quite favorable. However, neither of the approaches used by Shaw gives a proportionality constant in agreement with the measurements. Consequently, the accuracy of the pseudo-steady state approximation for small frequency mass transfer fluctuation is still unknown.

RESULTS

Qualitative Features of Mass Transfer Fluctuations at the Wall

Figure 2 displays signals from two 0.0127 cm electrodes that were 0.0457 cm (a dimensionless distance of $z = 18.1$) apart on the circumference of the pipe. The period associated with the mean frequency (1.87 Hz) calculated from the spectrum of the mass transfer fluctuations is shown along with the mean period of the velocity fluctuations measured by Lee (1972) and the bursting frequency reported by Klein et al. (1967) and Rao et al. (1971). It is noted that the frequency of the mass transfer fluctuations is an order of magnitude lower than that for the velocity fluctuations.

Of particular interest is the lack of correlation between the mass transfer rate at locations so close together on the pipe wall. On some short time spans, the two traces in Figure 2 can be superimposed on one another, but in other time spans they are directly opposite each other. This would indicate that variations approximately equal to the average mass transfer rates occurred over a distance of the order of 0.0457 cm. This lack of correlation between the two signals is indicated by a measured value of the correlation coefficient of 0.0015.

The association of such a small spatial scale with a turbulence quantity having such a low frequency is, as noted earlier, a surprising aspect of the mass transfer fluctuations observed at a wall.

Influence of Electrode Size

A series of experiments was conducted with electrodes of different sizes to determine how the measurements are affected by nonuniform flow over the electrode surface. Figure 3 shows the influence of the dimensionless electrode diameter 2a on the intensity of the mass transfer fluctuations. From the fall off of the intensity, it is concluded that averaging is important for $2a > 10$. This finding is consistent with the circumferential correlation measurements, which show that the first zero crossing occurs at $z \cong 20$.

Spectral measurements obtained with electrodes having diameters of 0.0125, 0.0211, and 0.0643 cm are compared in Figure 4. Here the spectral density function is normalized with $\overline{K_z^{+2}}$, and measurements for $2a = 8.81$ and $2a = 19.2$ are for an electrode with a diameter of 0.0125 cm. An influence of electrode size is noted for $2a > 10$. Figure 5 shows the same results with the spectral density function normalized by $\overline{k^{+2}}$. It is of interest that no significant influence of electrode size is observed when the measurements are correlated in this way. This result is surprising, since it suggests that the distribution of scales associated with the mass transfer fluctuations is independent of frequency.

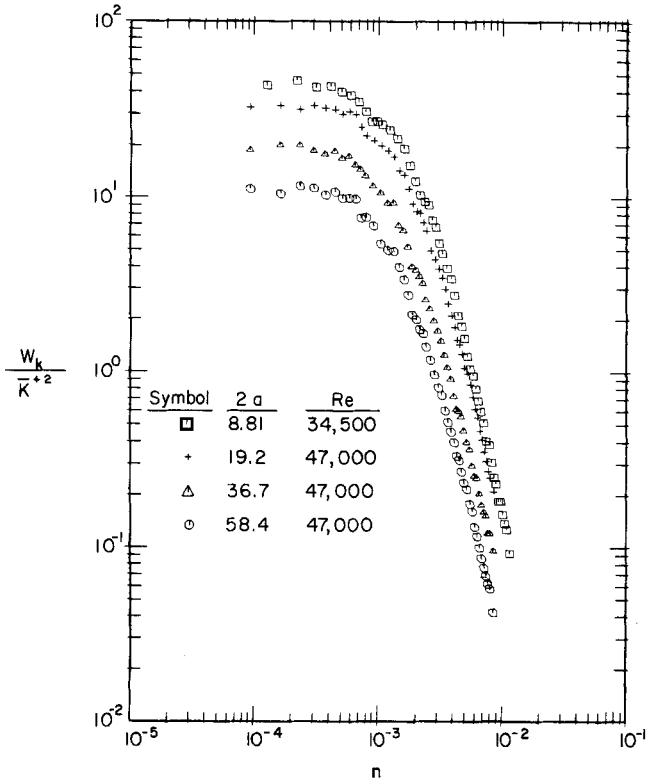

Fig. 4. Effect of 2a on the mass transfer spectra for Schmidt number = 695.

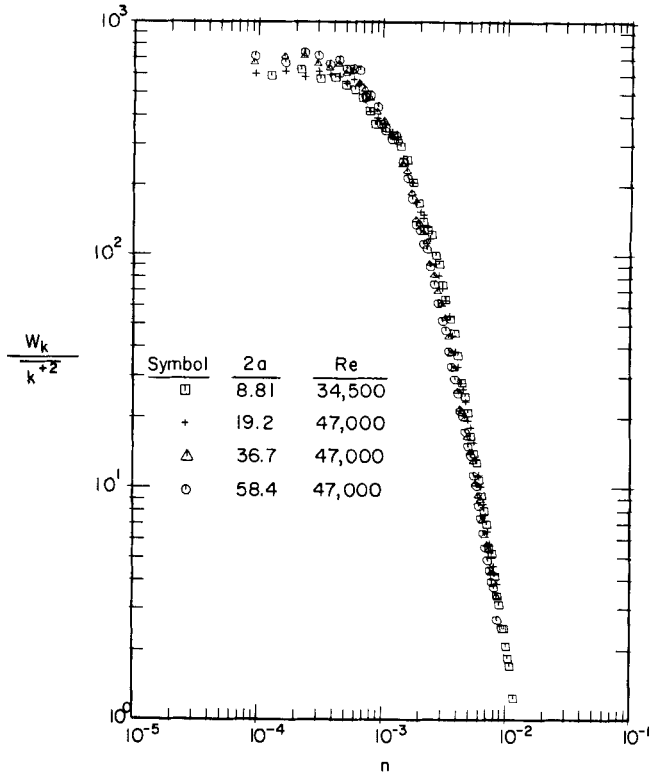

Fig. 5. Effect of electrodes size on the mass transfer spectra.

Use of the Similarity Assumption to Correlate Spectral Data

Twenty five spectra were measured for eleven Schmidt numbers ranging from 695 to 37 200. Figure 6 shows that the measurements were very reproducible. As was expected from dimensional analysis, and from the arguments presented in the theory section, the spectra are independent of Reynolds number when normalized with wall parameters.

The Schmidt number has a strong effect on the frequency of the mass transfer fluctuations. As shown in Figure 7, an increase in Schmidt number is associated with a marked diminution in the frequency of the mass transfer fluctuations. However, it has been found that the shapes at different Schmidt numbers are the same. This is illustrated in Figure 8, where the spectra are plotted as suggested by (5) using similarity parameter $Sc^{0.41}$.

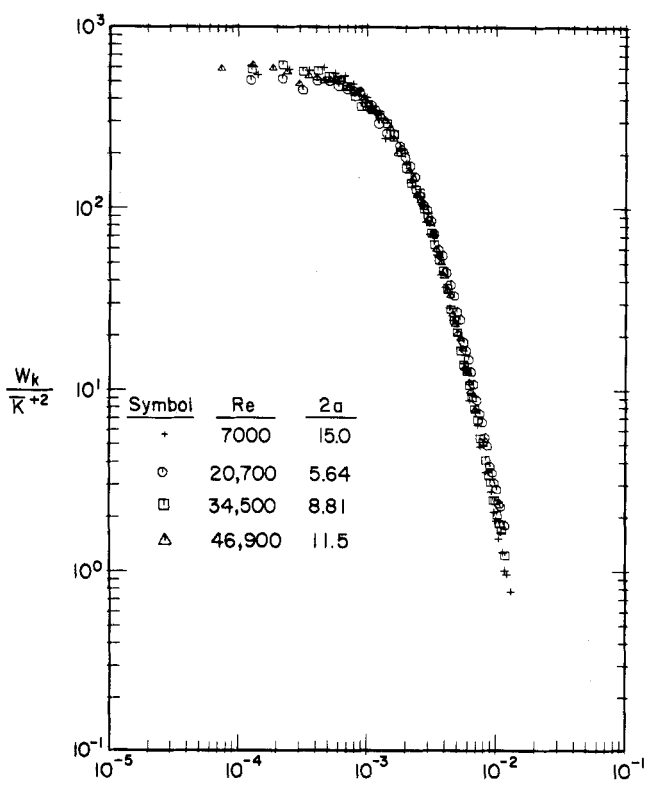

Fig. 6. Effect of Reynolds number on the mass transfer spectra for Schmidt number = 695.

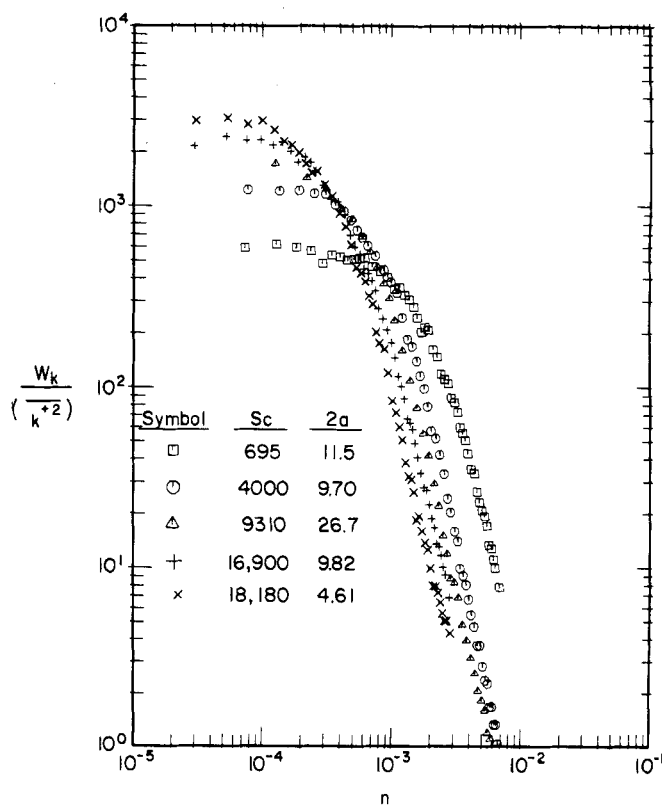

Fig. 7. Effect of Schmidt number on the mass transfer spectrum.

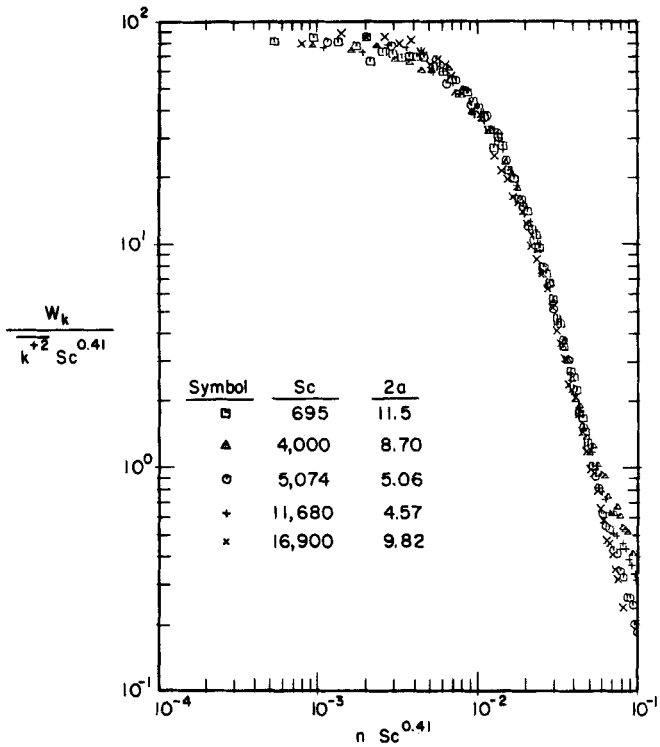

Fig. 8. Spectra plotted to show similarity in shape.

The exponent on the Schmidt number used in this similarity plot was determined by considering the influence of Schmidt number on the mean frequency $<n>$ and on the limiting value of the spectral density function at low frequencies W_1. The mean frequency defined as

$$<n> = \frac{1}{\overline{k^{+2}}} \int_0^\infty n\, W_k\, dn \qquad (35)$$

was determined numerically for each of the measured spectrum. The influence of Schmidt number on $<n>$ is shown in Figure 9, where the relation

$$<n> = 0.0215\, Sc^{-0.404} \qquad (36)$$

was determined by a least-squares fit. Figure 10 shows the influence of Schmidt number on W_1. The line through the data

$$\frac{W_1}{\overline{k^{+2}}} = 40\, Sc^{0.414} \qquad (37)$$

is a least-squares fit. The exponent $p = 0.41$ in the similarity plot was chosen as an average of the exponents appearing in (36) and (37).

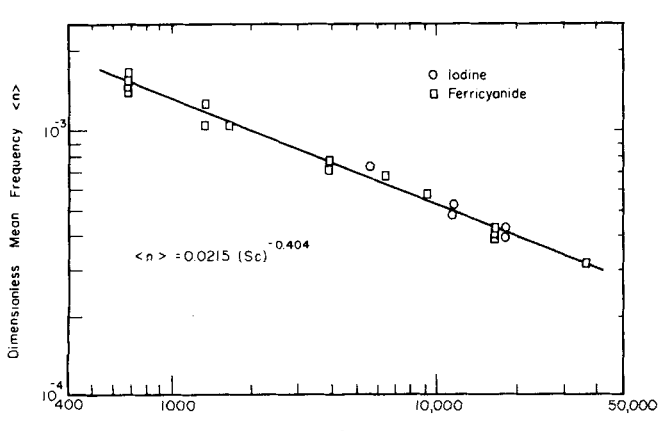

Fig. 9. Mean frequency of mass transfer fluctuations.

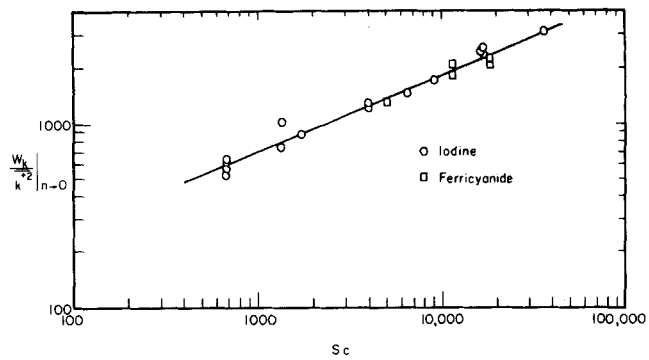

Fig. 10. The limit of the spectra for low frequency as a function of Schmidt number.

Comparison of the High Frequency Spectral Measurements with Linear Theory

Over the range of frequencies at which the mass transfer fluctuations were observed, the spectral functions for the velocity fluctuations close to a wall have been found to be constant (Sirkar and Hanratty, 1970). Consequently, the linear analysis proposed by Sirkar and Hanratty (1970) would suggest that at high frequencies a plot of $W_k/\overline{K^{+2}}$ vs. $n\ Sc^{1/3}$ should be independent of Schmidt number. Figure 11 shows several of the spectra plotted in this manner. Since the spectral density functions normalized with $\overline{K^{+2}}$ are greatly affected by electrode size, only spectra for which $2a < 12$ are considered.

It is to be noted that, as predicted by linear theory, the spectra for different Schmidt numbers come together at large frequencies when plotted in this manner. The line drawn through the data points has a slope of -3 and agrees with (29) if W_v is taken as 9.8×10^{-3}.

As shown by (30) and (31) in the theory section, agreement of the spectra with the similarity hypothesis and with linear theory for high frequencies requires that

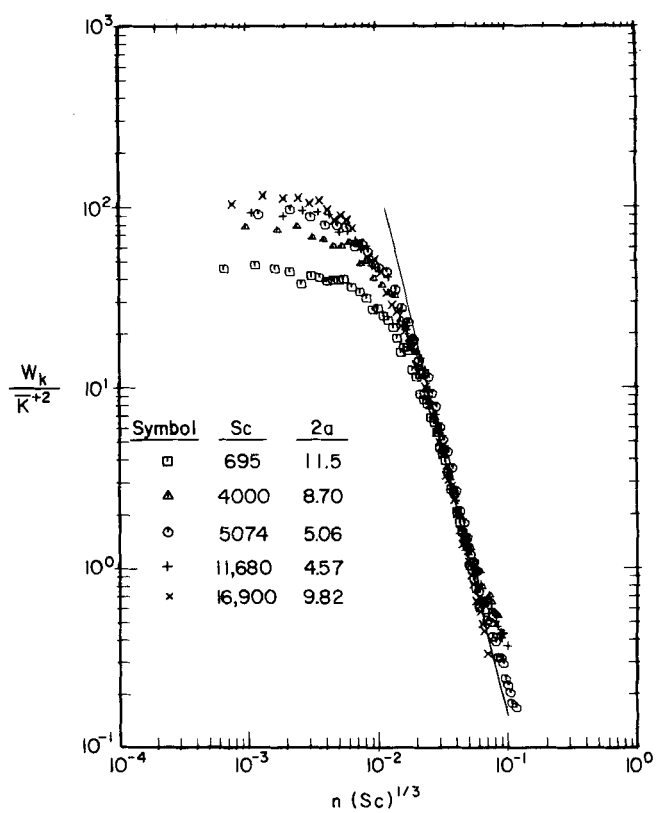

Fig. 11. Spectra plotted according to linear theory.

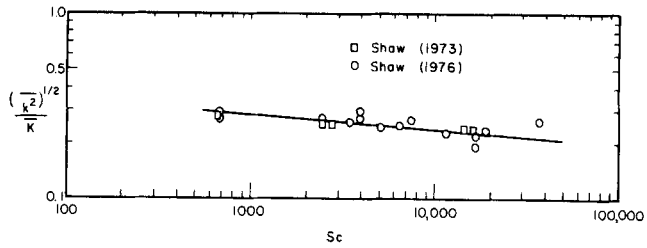

Fig. 12. Variation of mass transfer intensity with Schmidt number for $2a < 10$.

$$\frac{(\overline{k^2})^{1/2}}{\overline{K}} \sim Sc^{(2p-1)} = Sc^{-0.09} \qquad (38)$$

The above relation is compared with measurements of the relative intensity in Figure 12 for $2a < 10$. Unfortunately, the measurements of the relative intensity were rather scattered, so that it can only be said that this relation does not disagree with the measurements. The equation for the line shown in the figure is

$$\frac{(\overline{k^2})^{1/2}}{\overline{K}} = 0.54\, Sc^{-0.09} \qquad (39)$$

Correlation Measurements

The correlation coefficient, defined as

$$R_{kz} = \frac{\overline{k(o)\,k(z)}}{\overline{k^2}} \qquad (40)$$

for electrodes separated by a distance z in the lateral direction, was measured at four Schmidt numbers using the ferricyanide reaction. The results are presented in Figures 13 and 14. As indicated in Figure 13, the influence of spatial distance on the correlation coefficient does not depend on Schmidt number.

The mass transfer correlations are compared to velocity correlations in Figure 13. Note that the first zero crossing for the mass transfer comes at a z distance that is about half of that for the velocity correlation. Also, the location of the second zero crossing agrees approximately with that measured for the velocity correlation.

Figure 14 compares the variation of the correlation coefficient of the mass transfer fluctuations in the transverse direction measured in this research with the variation in axial direction determined by Van Shaw (1963). These results indicate that the structure of the fluctuating mass transfer field is very elongated in the direction of flow, as had been noted earlier by Van Shaw.

DISCUSSION AND INTERPRETATION

As outlined earlier, the goals of this research have been to determine the influence of Schmidt number on the mass transfer fluctuations, to relate these mass transfer fluctuations in the velocity field close to the surface, and to provide further insight as to how turbulent convective motions close to a surface control the mass transfer rate.

The Influence of Schmidt Number on the Mass Transfer Fluctuations

The influence of Schmidt number on the frequency of the mass transfer fluctuations is well represented by the similarity assumption that spectral functions measured at different Schmidt numbers fall on a single curve if plotted as $W_k/\overline{k^{+2}}\,(Sc)^{0.41}$ vs. $n\,Sc^{0.41}$. This implies that the mean frequency $<n>$ decreases as $Sc^{-0.41}$ in agreement with the measurements, Equation (36).

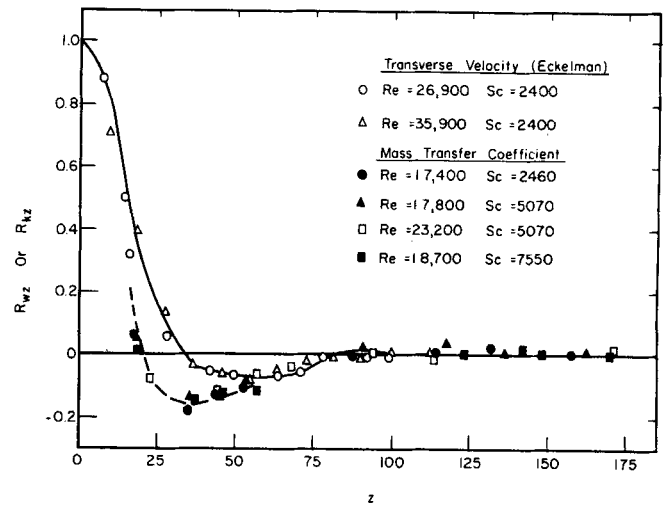

Fig. 13. Comparison of correlation coefficients for mass transfer and velocity fluctuations.

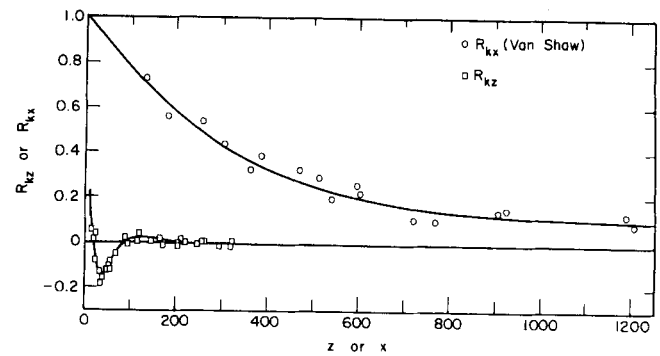

Fig. 14. Comparison of axial and transverse scales of mass transfer fluctuations.

Relation of the Mass Transfer Fluctuation to the Velocity Fluctuations

In trying to relate the mass transfer fluctuations to the velocity field, we have used the approach of Sirkar and Hanratty to seek asymptotic solutions valid for high and low frequencies. We find that the assumption that the high frequency fluctuations can be related to the velocity field by a solution of a linear form of the mass balance equation has considerable merit. We also find that the use of a pseudo steady state assumption to describe the asymptotic behavior of the spectral function requires an accurate evaluation of the nonlinear convective terms. Such an approach will probably require the incorporation of observations regarding the spatial structure of the turbulent concentration field. The correlation measurements show that the transverse scale of the mass transfer fluctuations is one-half to one times the transverse scale of the velocity fluctuations close to the wall. This suggests that the structure of the mass transfer field is dictated by the flow oriented eddies close to the wall. Yet, as shown in Figure 2, the period of the mass transfer fluctuations is an order of magnitude smaller than the period of these eddies. Furthermore, linear analysis shows that concentration fluctuations with frequencies of the order of the dominant velocity fluctuations would be highly damped in a region very close to the wall. This presents a paradox which is as yet unresolved.

One possible interpretation of these results is that the mass transfer fluctuations observed at the wall reflect the meandering of the flow oriented eddies described by a number of previous researchers. These flow oriented eddies are greatly elongated axially and on an average

have locations of maximum normal flow to the wall separated by a distance $\lambda/2$ in the lateral direction. These locations of maximum inflow or outflow would be where the turbulent transport is the greatest. Consequently, this interpretation would suggest that the lateral wavelength characterizing the spatial variation of the mass transfer rate would be one-half the lateral wavelength of the flow oriented eddies. This seems consistent with the measurements of the first zero crossing of the correlation coefficient.

Final Remarks Regarding the Mechanism of Mass Transfer

The picture of the mass transfer process which this tentative interpretation suggests is that the rate of mass transfer is controlled by convective motions in the flow oriented eddies. Molecular diffusion close to the surface greatly dampens the concentration fluctuations associated with these convective motions, so that the mass transfer fluctuations observed in the studies reported in this paper are not directly related to the Reynolds transport terms responsible for the turbulent convection of mass to the wall.

ACKNOWLEDGMENT

This work was partially supported by the National Science Foundation under Grant NSF ENG 71-02362.

NOTATION

A = area of the electrode
a = Radius of the electrode normalized with ν/v^*
A_c = constant defined by Equation (44)
b = constant defined by Equation (15)
C = local concentration ot the diffusing species normalized with C_B
$\overline{C}$ = time averaged value of C
c = fluctuation in the concentration normalized with C_B
$\hat{c}$ = amplitude of the concentration fluctuations normalized with C_B
$\tilde{c} = \dfrac{\hat{c}\,\omega^2\,Sc}{\hat{v}\left.\dfrac{d\overline{C}}{dy}\right|_0}$
$c^{++} = \dfrac{\hat{c}\,Sc^2\,\overline{K}^{+3}}{\hat{v}}$
$c^* = \dfrac{\hat{c}}{\hat{v}\,\overline{K}^+}$
C_B = bulk concentration of the diffusing species
D = diffusion coefficient, $cm^2\ s^{-1}$
F = Faraday's constant
I = electric current flowing in the electrolysis cell
K = mass transfer coefficient $= N/C_B$
$\overline{K}$ = time averaged mass transfer coefficient
K^+ = K/v^*
k = fluctuation in the mass transfer coefficient
k^+ = k/v^*
K_∞ = fully developed mass transfer coefficient
N = rate of mass transfer per unit area, mole $s^{-1}\ cm^{-2}$
n = frequency normalized with v^{*2}/ν
$\langle n \rangle$ = mean in frequency normalized with $\dfrac{v^{*2}}{\nu} = \dfrac{1}{\overline{k}^{+2}} \int n W_k\, dn$
n_e = number of electrons involved in the electrochemical reaction
Re = Reynolds number
$\overline{S}$ = time averaged velocity gradient at the wall
Sc = Schmidt number $= \nu/D$
s_x = x component of the fluctuating velocity gradient at the wall normalized with v^{*2}/ν
s_z = z component of the fluctuating velocity gradient at the wall normalized with v^{*2}/ν
t = time normalized with ν/v^{*2}
U = velocity in the x direction normalized with v^*
$\overline{U}$ = time averaged value of U
u = x component of the fluctuating velocity normalized with v^*
U_c = convection velocity normalized with v^*
v = y component of the fluctuating velocity normalized with v^*
$\hat{v}$ = amplitude function defined by Equation (21)
v^* = friction velocity $= (\nu\overline{S})^{1/2}$
w = transverse component of the fluctuating velocity normalized with v^*
W_k = spectral density function for k normalized with ν
W_v = spectral density function for $\hat{v}$ normalized with wall parameters, v^* and ν
W_1 = limiting value of W_k for $n \to 0$
x = coordinate in the direction of mean flow normalized with ν/v^*
y = coordinate in the direction perpendicular to the wall normalized with ν/v^*
$\tilde{y}$ = $y(\omega Sc)^{1/2}$
y^{++} = $y\,Sc\,\overline{K}^+$
y^* = $b^{1/n}\,Sc^{1/n}y$
z = coordinate transverse to the direction of mean flow normalized with ν/v^*

Greek Letters

δ_c = thickness of the boundary layer for c normalized with ν/v^*
δ_C = thickness of the boundary layer for $\overline{C}$ normalized with ν/v^*
ϵ = eddy viscosity $cm^2\ s^{-1}$
ϵ^+ = eddy viscosity normalized with ν
ν = kinematic viscosity
ω = circular frequency $= 2\pi n$

LITERATURE CITED

Eckelman, L. D., "The Structure of Wall Turbulence and its Relation to Eddy Transport," Ph.D. thesis, Univ. Ill., Urbana (1971).

Klein, S. J., W. C. Reynolds, F. A. Schraub, and P. W. Runstadler, *J. Fluid Mech.*, 30, 741 (1967).

Lee, M. K., "Method for Measuring Wavelength and Bursting Period of Flow Oriented Eddies in the Viscous Sublayer," M.S. thesis, Univ. Ill., Urbana (1972).

———, L. D. Eckelman, and T. J. Hanratty, "Identification of Turbulent Wall Eddies Through the Phase Relation of the Components of the Fluctuating Velocity Gradient," *J. Fluid Mech.*, 66, 17 (1974).

Morrison, W. R. B., K. J. Bullock, and R. E. Kronauer, "Experimental Evidence of Waves in the Sublayer," *ibid.*, 47, 639 (1971).

Rao, K. N., R. Narasimha, and M. A. Bodri Narayanan, *ibid.*, 48, 439 (1971).

Shaw, D. A., "Measurement of Frequency Spectra of Turbulent Mass Transfer Fluctuations at a Pipe Wall," M.S. thesis, Univ. Ill., Urbana (1973).

———, "Mechanism of Turbulent Mass Transfer to a Pipe Wall at High Schmidt Number," Ph.D. thesis, Univ. Ill., Urbana (1976).

———, and T. J. Hanratty, "Turbulent Mass Transfer Rates to

a Wall for Large Schmidt Numbers," *AIChE J.*, 23, 28 (1977).
Sirkar, K. K., "Turbulence in the Immediate Vicinity of a Wall and Fully Developed Mass Transfer at High Schmidt Numbers," Ph.D. thesis, Univ. Ill., Urbana (1969).
———, and T. J. Hanratty, "Relation of Turbulent Mass Transfer to a Wall at High Schmidt Numbers to the Velocity Field," *J. Fluid Mech.*, 44, 589 (1970).
Van Shaw, P., "A Study of the Fluctuation and the Time Average of the Rate of Mass Transfer to a Pipe Wall," Ph.D. thesis, Univ. Ill., Urbana (1963).
———, and T. J. Hanratty, "Fluctuations in the Local Rate of Turbulent Mass Transfer to a Pipe Wall," *AIChE J.*, 10, 475 (1964).

Manuscript received July 22, 1976; revision received November 17, and accepted November 19, 1976.

A Compartmental Dispersion Model for the Analysis of Mixing in Tube Networks

JAMES S. ULTMAN

Department of Chemical Engineering and The Bioengineering Program The Pennsylvania State University University Park, PA 16802

and

HAL S. BLATMAN

The Medical College of Pennsylvania Philadelphia, PA 19129

A compartmental dispersion model of longitudinal mixing in tube networks has been developed. The ability of this model to predict the impulse response of helium, benzene vapor, and sulfur hexafluoride tracer gases in two and in five generation symmetric network models of the large airway system of the lung has been tested over an air flow range of 1 to 400 ml/s.

The results imply that velocity profile distortion and secondary flows in branching regions have only a small effect upon the overall longitudinal mixing when flow is directed toward the higher-order generations. On the other hand, accurate prediction of the data requires adequate treatment of the finite rate of evolution of the Taylor dispersion occurring in these tube networks.

SCOPE

The tracer dispersion technique applied to both the cardiovascular and pulmonary systems has become an accepted, if not routine, method of diagnosis and function testing. In the lungs especially, where there are several reliable models of the flow network geometry (see, for example, Weibel, 1963; Horsfield and Cumming, 1968*a*), it should be possible to predict the tracer dispersion from first principles. Or, what is the more relevant biomedical problem, given a set of tracer dispersion data, it might be possible to recognize the nature of deviations in the system geometry from an established norm.

The objective of this study was to develop an approximate method of predicting tracer dispersion for laminar flow through a tube network of known geometry. Though attention was focused upon symmetrically branched models of the pulmonary airway system, the methods can be extended to other tube networks as well.

Although a wealth of pulmonary dispersion data obtained from human subjects exists, its interpretation has led to inconsistent conclusions among the various investigators. For example, following a 60 ml inspiration of a helium-oxygen mixture, Briscoe et al. (1954) found detectable levels of helium in the gas sampled between 750 and 1 250 ml expired. These investigators concluded that the convective displacement of the helium in a parabolic front must be responsible for its unexpectedly high penetration. Power (1969) repeated the same experiment using a mixture of hydrogen and sulfur hexafluoride in air and concluded that molecular diffusion was of primary importance since the helium consistently penetrated deeper than the sulfur hexafluoride.

The principal source of confusion in these studies stems from an oversimplified analysis of the data. In particular, we feel that in analyzing pulmonary airway transport, one must allow for significant contributions from several simultaneous mixing modes. Wilson and Lin (1970) made this point by estimating the relative importance of various tubular mixing mechanisms in Weibel's (1963) symmetric model of lung geometry; in this model, the pulmonary tree is comprised of a set of twenty-three generations of bifurcating tubes originating at the trachea. Wilson and Lin's computations indicate that transport by pure convection is most important in the upper eight pulmonary airway generations, Taylor dispersion becomes significant in the following four generations, while axial diffusion is an important factor in the last eleven generations. Thus, in developing an algorithm for predicting tracer dispersion in the lungs, we have attempted to simultaneously account for gas transport by convection, axial dispersion, and axial diffusion.

Correspondence concerning this paper should be addressed to James S. Ultman.